

RESEARCH ARTICLE

Molecular cloning and expression profiling of a chalcone synthase gene from *Lamiophlomis rotata*

QIAO FENG^{1*}, GENG GUI-GONG², ZENG YANG¹, XIE HUI-CHUN¹, JIN LAN¹, SHANG JUN¹ and CHEN ZHI¹

¹Lab of Environment and Resource in Qinghai-Tibet Plateau, Ministry of Education, Qinghai Normal University, Xining 810008, People's Republic of China

²Laboratory of Quality and Safety Risk Assessment for Agro-products, Ministry of Agriculture, Xining 810016, People's Republic of China

Abstract

Lamiophlomis rotata is a renowned Chinese medicinal plant. Chalcone synthase (CHS) is important in flavonoid and isoflavonoid biosynthesis, catalysing the formation of naringenin chalcone in plants. A full-length cDNA encoding the *CHS* gene was cloned from *L. rotata* based on the highly conserved *CHS* gene sequences of *Labiatae* plants. A blast search showed its homology (named *LrCHS*) with other *CHS* genes of *Labiatae* plants. The full-length genomic DNA of *LrCHS* was 2026 bp with one intron of 651 bp, two exons of 178 bp and 998 bp, flanked by a 73 bp 5'-UTR and a 126 bp 3'-UTR. The cDNA sequence of the *LrCHS* gene had an 1176 bp open reading frame encoding a 391 amino acid protein of 42,798 Da. The CHS protein predicted from *L. rotata* showed 79–86% identity with CHS of other plant species. We conducted a phylogenetic analysis of nine families containing 48 plants and *L. rotata* based on the full amino acid sequences of CHS proteins. Consequently, *LrCHS* was located in the *Labiatae* branch. Additionally, we examined *LrCHS* gene expression patterns in different tissues by quantitative real-time PCR with specific primers. The expression analysis showed preferential expression of *LrCHS* in flowers and leaves during the flowering stage. Total flavonoid content and *CHS* gene expression exhibited similar patterns during *L. rotata* organ development. In agreement with its function as an elicitor-responsive gene, *LrCHS* expression was coordinated by methyl jasmonate and UV light, and induced between 6 and 18 h. These results provide a molecular basis for additional functional studies of *LrCHS* in *L. rotata*.

[Feng Q., Gui-Gong G., Yang Z., Hui-Chun X., Lan J., Jun S. and Zhi C. 2015 Molecular cloning and expression profiling of a chalcone synthase gene from *Lamiophlomis rotata*. *J. Genet.* **94**, 193–205]

Introduction

Flavonoids and isoflavonoids are major flower pigments in plants and are involved in many aspects of plant growth and development, such as pathogen resistance, pigment production, UV light protection, pollen growth and seed coat development (Heller and Hahlbrock 1980; Hahlbrock 1981; Dao *et al.* 2011; Abdel-Lateif *et al.* 2013; Dare and Hellens 2013). A key enzyme for flavonoid and isoflavonoid biosynthesis is chalcone synthase (CHS, EC 2.3.1.74), which catalyses naringenin chalcone formation (figure 1 of Hahlbrock 1981). Many genes encoding CHS have been cloned, sequenced and characterized from various plant species (Dooner 1983; Alfred *et al.* 1991; An *et al.* 1993; McKhann and Hirsch 1994; Nakajima *et al.* 1996; Pang *et al.* 2004; Jiang *et al.* 2006; Lu *et al.* 2009; Pitakdantham *et al.* 2010).

Chalcone synthases provide the starting materials for a diverse set of metabolites such as flavonoids (figure 1), which

play differential roles in flowering plants, including that of providing floral pigments, antibiotics, UV protectants and insect repellents (Hahlbrock and Scheel 1989). Flavonoids have been identified as plant signals and developmental regulators in legume nodulation, and are thought to play a critical role during actinorhizal nodulation (Abdel-Lateif *et al.* 2013). Flavonoids also benefit human, as they exhibit—amongst other functions—cancer chemoprevention (Jang *et al.* 1997), antimitotic (Edwards *et al.* 1990), oestrogenic (Gehm *et al.* 1997), antimalarial (Li *et al.* 1995), antioxidant (Jang *et al.* 1997), and antiasthmatic (Zwaagstra *et al.* 1997) activities. Due to their high antioxidant capacity, increasing evidence suggests that flavonoids might offer health-protecting components in the human diet (Sugihara *et al.* 1999; Dugas *et al.* 2000). Anthocyanins have been used therapeutically against cardiovascular diseases, cancer (Trevisanato and Kim 2000) and age-related conditions like Alzheimer's disease (Commenges *et al.* 2000). Due to increasing health problems in many parts of the world, ways to commercially produce antioxidants in commercial foods should contribute significantly to human health.

*For correspondence. E-mail: qiaofnm@163.com.

Keywords. chalcone synthase; quantitative real-time PCR; *Lamiophlomis rotata*.

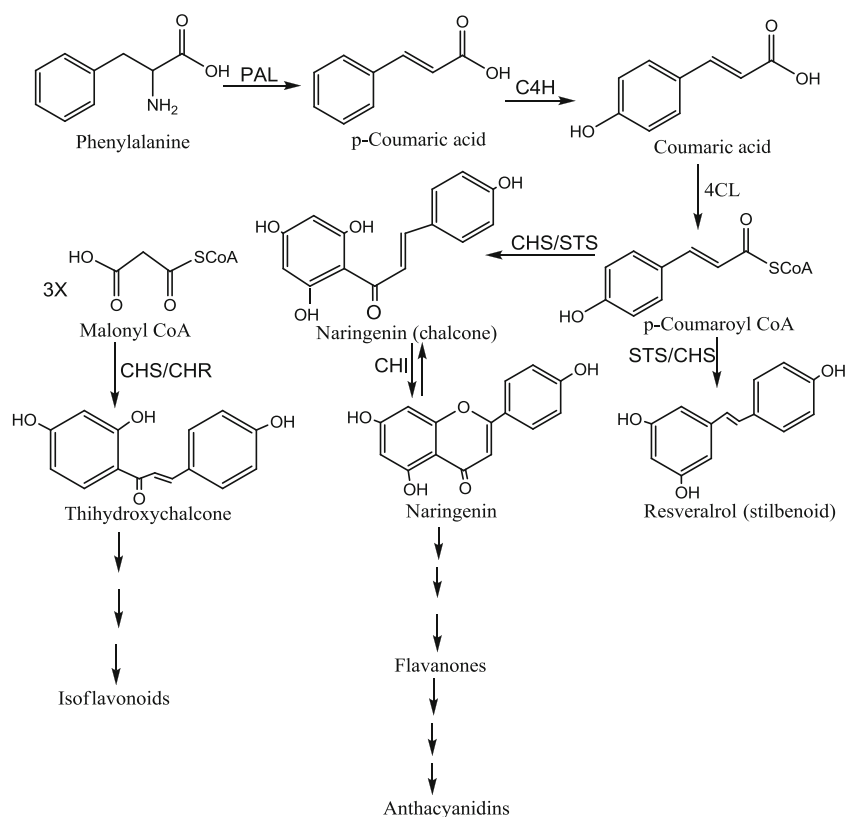


Figure 1. Flavonoid biosynthetic pathway. PAL, phenylalanine ammonia-lyase; C4H, cinnamate-4-hydroxylase; CHR, chalcone reductase; STS, stilbene synthase; CHI, chalcone isomerase.

L. rotata is a well-known medicinal plant in the Qinghai–Tibet Plateau that belongs to the *Lamiophlomis* genus and family Lamiaceae. We identified 67 chemical components in the natural *L. rotata* population by gas chromatography–mass spectrometry (GC–MS) (Liu 2006). Iridoid glycosides and flavonoids are two effective components of *L. rotata* (Lü et al. 2012). Since CHS catalyses the first committed step in flavonoid biosynthesis, it has been widely studied since its discovery. Therefore, it is necessary to explore *L. rotata*'s structure and expression.

Here, we describe the cloning of CHS cDNA from *L. rotata*, deriving evolutionary relationships between the studied species and other plants. We have also studied the sequence and expression of the *CHS* gene in *L. rotata*. Chalcone synthase catalyses the initial step in flavonoid synthesis, and *CHS* from *L. rotata* affects the flavonoid content that performs important physiological activities. Based on the cloning and characterization of the *CHS* gene from *L. rotata*, researchers have obtained additional genetic information which was linked to some of *L. rotata*'s pharmacological effects.

Materials and methods

Plant materials

L. rotata was grown in the natural pastures of Yushu (Qinghai, China) with an average altitude of 4500–5000 m.

Before initiating experiments, we collected young leaves to isolate genomic DNA and total RNA. We also collected leaves, stems, petioles, roots and flowers from the same plants, and immediately immersed them in liquid nitrogen in the flowering stage for RNA isolation and detecting CHS mRNA expression.

DNA and RNA extractions, and RT-PCR

We extracted genomic DNA from fresh leaves using CTAB (Murray and Thompson 1980). RNA was isolated using Trizol reagent (Invitrogen, Shanghai, China) from leaves, stems, petioles, roots and flowers of *L. rotata*. Samples were pretreated with RNase-free DNase I (Takara, Dalian, China) to remove contaminated genomic DNA. Total RNA was used in primary genetic molecular cloning and expression profiling. Reverse transcription was performed on 1 µg RNA samples using an AMV First Strand cDNA Synthesis kit (Takara, Dalian, China). The first cDNA strand was stored at –20°C.

cDNA sequences were PCR amplified for CHS using specific primers (table 1). First, ~500-bp CHS cDNA fragment was amplified with the primers DCHS5F/DCHSQR1, followed by PCR amplification of ~700 bp fragment with the specific primers DCHSQF1/DCHSQR2. Subsequently, ~1200 bp fragment was obtained that covered the previous two fragments. Amplifications were performed with 1 µM of each primer in 3 mM MgCl₂, 20 µM of each

dNTP and 1.25 units of LA *Taq* polymerase (Takara, Dalian, China) in a total volume of 20 μ L of a 1 \times reaction buffer. PCR cycles included an initial denaturation at 95°C for 3 min, followed by 35 cycles of denaturation at 94°C for 40 s, an annealing step at 58°C for 40 s, and an elongation step at 72°C for 45 s, followed by a final elongation step at 72°C for 10 min. All amplified products with DCHS5F/DCHSQR1, DCHSQF1/DCHSQR2 and DCHSQF1/DCHSQR2 were inserted into pMD18-T cloning vectors (TaKaRa, Dalian, China) and transformed into chemically competent *Escherichia coli* JM109 cells (Sunbiotech, Beijing, China) according to the manufacturer's instructions (Promega, Beijing, China). Recombinant colonies were screened for inserts of the expected size using standard methods and PCR amplification with M13-47/M13-48 primers (Sunbiotech, Beijing, China). We sequenced 3–4 selected clones (Sunbiotech, Beijing, China) using the same primers. The sequences were compared with those found in the NCBI database using BLAST and similar sequences were aligned using CLUSTAL, ver. 1.83.

Rapid amplification of cDNA 3' end and cDNA 5' end

cDNA synthesis using the 3'-full RACE Core Set ver. 2.0 (TaKaRa, Dalian, China) was performed for 3' rapid amplification of cDNA ends. RNA was reverse transcribed with a cDNA synthesis primer AP (that was provided in the kit). Two specific primers, DCHS3R1 and DCHS3R2 (table 1), were designed based on the conserved sequence of *LrCHS*. Subsequently, 3' RACE-PCR with the DCHS3R1 primer and the 3' RACE-PCR outer primer (that was provided in the kit)

in the first round of the PCR assay was followed by PCR using the DCHS3R2 primer and the 3' RACE-PCR inner primer (provided in the kit) for the second round. The final PCR products were separated on a 1.2% agarose gel stained with ethidium bromide. The target DNA band was purified using a DNA Purification Kit (Sunbiotech, Beijing, China), and ligated to the pMD18-T vector (TaKaRa, Dalian, China), followed by transformation in *E. coli* JM109 (Sunbiotech, Beijing, China) with a heat-shock (42°C, 1 min) method. At least five of the positive clones that were confirmed by PCR were then sequenced using M13-47/M13-48 primers (Sunbiotech).

To clone the 5' end, we designed primers of DCHSQR1 and DCHSYR1 (table 1) based on the sequencing results of 5' end and conserved sequences. We performed 5'-RACE-PCR using the 5'-full RACE kit (TaKaRa, Dalian, China). RNA was dephosphorylated, decapped and ligated to the 5' RACE Adaptor following the kit's protocol. Subsequently, RT-PCR was performed using Random 9-mer primers (provided in the kit). This fragment was extended by 5' -RACE using DCHSQR1 (outer primer) and 5'RACE-PCR outer primer (provided in the kit) in the first round of the PCR. We then used DCHSYR1 (inner primer) and 5'RACE-PCR inner primer (provide in the kit) for the second round of PCR. The second PCR product was separated on a 1.2% agarose gel, extracted and recovered and ligated to the pMD18-T vector (TaKaRa, Dalian, China), transformed into *E. coli* JM109 (Sunbiotech, Beijing, China) and sequenced as described in the 3'-RACE-PCR cloning.

Table 1. Primer sequences in this study.

Primer	Purpose	Primer sequence (5'–3')	Location in ORF of <i>LrCHS</i>
DCHS5F (forward)	cDNA sequence of CHS	ATGGTGAC(C/A)GT(G/C/T)GA(G/A)GA(A/C)(A/T)(T/A)CC	1–19
DCHSQR1 (reverse)*	cDNA sequence of CHS; 5'RACE (outer primer)	AGCAGCCCTGCTGGTACATCATGAA (–550)	469–493
DCHSQF1 (forward)	cDNA sequence of CHS	TTCATGATGTACCAGCAGGGCTGCT	469–493
DCHSQR2 (reverse)	cDNA sequence of CHS	AC(C/G)GTGAGGCCCGG(C/G)CCGAA	1117–1136
DCHS3R1 (forward)**	3'RACE (outer primer)	GACATGTGTTGAGTGAATATGG	975–996
DCHS3R2 (forward)**	3'RACE (inner primer)	GTCGAGTAGACATGTGTTGAGT	983–1004
DCHSYF1 (forward)	Real-time PCR	AAGATCACCCACCTCGTCTTCTG	367–389
DCHSYR1 (reverse)*	Real-time PCR; 5'RACE (inner primer)	GCTGGTACATCATGAAGCGTTTG	484–462
PCHSWF1 (forward)	Full cDNA/genomic DNA fragment of CHS	CGTCGAAAATGGTGACCGTGGA	–8–14
PCHSWR1 (reverse)	Full cDNA/genomic DNA fragment of CHS	CCCGTAGTCAAATTAAGTAACC	1177–1201
DACTINF1 (forward)	cDNA sequence of ACTIN	GT(G/C)GCTCC(T/A)GAAGAGCA	
DACTINR1 (reverse)	cDNA sequence of ACTIN	CTC(A/G)GCAGT(G/T)GTGGT(G/A)AA	

Generating the full length cDNA and genomic DNA sequence

By aligning the RT-PCR, 3'-RACE-PCR and 5'-RACE-PCR product sequences using Clustal W software, we deduced and analysed the full-length *LrCHS* cDNA. Two gene-specific primers, PCHSWF1 and PCHSWR1, which covered the start and stop codons, respectively, were designed to obtain full-length cDNA and the genomic DNA sequence of *LrCHS*. To obtain genomic DNA, we monitored the extension time during the amplification cycles from 1.5 to 3 min. We repeated the PCR amplification and sequencing for the full-length cDNA and genomic *LrCHS* DNA thrice. The PCR product was separated on a 1.2% agarose gel, extracted and recovered, ligated to the pMD18-T vector (TaKaRa, Dalian, China), and transformed into *E. coli* JM109 (Sunbiotech, Beijing, China). At least six of the positive clones, as performed in the full gene cloning, were sequenced using M13-47/M13-48 primers (Sunbiotech).

Analysis of CHS coding sequences

LrCHS sequences from *L. rotata* were compared using BLASTn from NCBI, and similarity analyses used Clustal W software in the BioEdit 7.0.5.2 package. The amino acid sequences were aligned using BLASTx from NCBI. Exon/intron regions were identified using Gene-Seqer and matched with the full-length cDNA sequences for each gene using Clustal W software. We performed an analysis of primary structures from deduced amino acid sequences using Clustal W and edited them with the BoxShade toolset (3.21, EMBnet, Switzerland). The full-length cDNA sequences were submitted to NCBI's GenBank with the following GenBank accession number: *LrCHS*, KM114220.

Bioinformatics and phylogenetic analyses

The obtained sequences were analysed using BLAST (<http://blast.ncbi.nlm.nih.gov/Blast.cgi>). Multialignment of CHS amino acid sequences was done using Clustal W software. We predicted the molecular weight, isoelectric point (pI) and structural analysis of the deduced *LrCHS* protein using the ExPASy Proteomics Server (<http://www.expasy.org/>). We employed SOSUI (<http://azusa.proteome.bio.tuat.ac.jp/sosui/>) to analyse the solubility of *LrCHS* and we predicted subcellular *LrCHS* localization using WoLF PSORT (<http://www.psort.org/dataset/index.html>). Functional site predictions were determined using ELM (<http://elm.eu.org/>). We performed phylogenetic analyses by aligning the *LrCHS* amino acid sequence and other CHS protein sequences that were retrieved from GenBank using Clustal W software (Thompson et al. 1997).

Multiple alignments of the putative amino-acid sequence of *L. rotata* CHS and nine plants were done using the DNAssist 2.0 program. Construction of the phylogenetic tree included the sequences for the *L. rotata* CHS protein and/or putative CHS proteins reported in the NCBI database for

48 plants (table 2). Protein sequences were aligned using Clustal W (Thompson et al. 1997). We built the molecular phylogenetic tree for CHS with neighbour-joining (NJ) and maximum-parsimony methods, using Poisson correction as an amino acid model in the MEGA program (software ver. 4.0). Bootstrap values were derived from 1000 replicates (Thompson et al. 1994).

Gene expression analyses with quantitative real-time PCR

Quantitative real-time PCR (qRT-PCR) reactions were performed with an iCycler iQ Multicolor Real-Time PCR Detection system (Bio-Rad, Shanghai, China) using iQ SYBR Green Supermix (Takara, Dalian, China) to monitor cDNA amplification, according to the manufacturer's protocol. According to the conserved *ACTIN* gene sequence in several Labiatae plants, the degenerate primers DACTINF1 and DACTINR1 that were used to amplify the *ACTIN* gene from *L. rotata* were designed and amplified for a fragment length of 330 bp (GenBank number KF438040). The primers used were: DACTINF1: GT(G/C)GC TCC(T/A)GAAGAGCA; DACTINR1: CTC(A/G)GCAGT (G/T)GTGGT(G/A)AA. Quantitative analysis of *ACTIN* gene fluorescence was used to sequence the design of specific primers DACTINYF1 and DACTINYR1, and the expected amplification fragment length was 95 bp. The gene-specific *CHS* primers DCHSYF1 and DCHSYR1 (table 1) were used for real-time PCR, yielding a product of 118 bp. The actin primers DACTINYF1 and DACTINYR1 (table 1) were used for reference, yielding a product of 95 bp. We performed qRT-PCR using the iQ SYBR Green Supermix (Bio-Rad) on an iQ-Cycler (Bio-Rad) under the following conditions: an initial denaturing cycle for 2 min at 95°C, followed by 40 cycles of successive denaturation, annealing and polymerization reactions (20 s at 95°C, 30 s at 60°C and 30 s at 72°C). PCR amplification was conducted in a 25 µL total volume containing 3 µL of diluted cDNA, 0.5 µM of each primer, and 11 µL of 2x iQ SYBR Green Supermix. In each experiment, the target and control samples were amplified in the same plate with a series of diluted cDNA (1×10^5 – 1×10^{11} copies per µL) to generate calibration-specific curves. We performed three to four independent experiments for each sample. After performing qRT-PCR, we confirmed the absence of unwanted byproducts by an automated melting curve analysis and agarose gel electrophoresis of the PCR products.

In all experiments, three replicates for each RNA sample were included; averages were calculated, and differences in the threshold cycle (Ct) were evaluated. We used the comparative Ct method, which mathematically transforms the Ct data into the relative transcription level genes. When comparing CHS expression in different tissues, we achieved the relative quantification of *LrCHS* expression by calibrating its transcription level to that of the reference house-keeping gene *ACTIN*, which enabled presentation of the relative amounts of the *LrCHS* transcript as $2^{-(\Delta Ct)}$ according to

Table 2. Species and Genbank accession numbers of CHS protein sequences in some plants.

Family	Species	GenBank accession number
Poaceae	<i>Triticum aestivum</i>	AAQ19322.1
	<i>Thinopyrum ponticum</i>	AAQ19319.1
	<i>Secale cereale</i>	CAA63305.1
	<i>Hordeum vulgare</i>	CAA41250.1
	<i>Oryza sativa</i>	NP_001068009.1
Polygonaceae	<i>Fagopyrum tataricum</i>	ACZ51475.1
	<i>Fagopyrum dibotrys</i>	ACZ48699.1
	<i>Persicaria minor</i>	AFI98395.1
	<i>Rheum palmatum</i>	ABB13608.1
Umbelliferae	<i>Polygonum cuspidatum</i>	AFD64563.1
	<i>Daucus carota</i>	BAA03784.1
	<i>Petroselinum crispum-1</i>	CAA24779.1
	<i>Petroselinum crispum-2</i>	PRF223820
Brassicaceae	<i>Cardamine pratensis</i>	AAG43358.1
	<i>Ionopsidium abulense</i>	AAG43360.1
	<i>Arabidopsis thaliana</i>	AED91961.1
	<i>Brassica oleracea</i>	AAO73441.1
Rosaceae	<i>Sisymbrium irio</i>	AAG43359.1
	<i>Prunus persica</i>	AFJ49141.1
	<i>Rosa hybrid cultivar</i>	BAC66467.1
	<i>Malus toringoides</i>	ADV29810.1
Leguminosae	<i>Pyrus communis</i>	AGL81345.1
	<i>Senna alata</i>	AAM00232.1
	<i>Vigna unguiculata</i>	CAA52819.1
	<i>Arachis hypogaea</i>	AAU43217.1
	<i>Lupinus luteus</i>	AAP37052.1
	<i>Glycyrrhiza inflata</i>	ACH67480.1
Solanaceae	<i>Medicago sativa</i>	L02901.1
	<i>Onobrychis viciifolia</i>	AAB81987.1
	<i>Petunia x hybrida</i>	AAB36038.1
	<i>Brunfelsia brasiliensis</i>	AEW12813.1
	<i>Nicotiana glauca</i>	ACS12837.1
	<i>Solanum tuberosum</i>	AEN83501.1
Labiatae	<i>Solanum lycopersicum</i>	NP_001234036.1
	<i>Nierembergia</i>	BAC10998.1
	<i>Perilla frutescens</i>	BAA19656.1
	<i>Solenostemon</i>	ABP57071.1
	<i>scutellarioides</i>	
	<i>Agastache rugosa</i>	AFL72079.1
Scrophulariaceae	<i>Lamiophlomis rotata</i>	KM114220
	<i>Scutellaria baicalensis-1</i>	AAB88208.1
	<i>Scutellaria baicalensis-2</i>	ABS83551.1
	<i>Scutellaria viscidula</i>	ACC68839.1
	<i>Mazus pumilus</i>	AAN05791.1
	<i>Digitalis lanata</i>	CAA05512.1
	<i>Digitalis2 lanata</i>	CAA05512.1
	<i>Misopates orontium</i>	CAJ44127.1
Antirrhinum	<i>Antirrhinum majus-1</i>	BAM29292.1
	<i>Antirrhinum majus-2</i>	BAM29290.1
	<i>Antirrhinum3 majus</i>	CAA27338.1

the C_T method ($dCt = C_{t_{sample}} - C_{t_{control}}$), as described in the qRT-PCR Application Guide (TaKaRa, Dalian, China). When comparing *LrCHS* expression in different tissues, we achieved the relative *LrCHS* expression by calibrating its transcription level to that of the reference gene, *ACTIN*.

Determining total flavonoid contents

We ground up different organizations (2–3 g) of the flowering stage of *L. rotata* in liquid nitrogen and extracted the samples in 2% hydrochloric acid in methanol for 24 h and in the dark at room temperature. After centrifugation at 8000 g for 20 min at 4°C, we diluted the supernatant to assay total flavonoids which were measured as previously described (Wolfe *et al.* 2003). Absorption values were analysed at a wavelength of 510 nm, and the results were expressed as mg (catechin)/g (fresh weight).

Plant material treated with elicitor

L. rotata seeds were surface-sterilized in 1% NaClO for 10 min and soaked in water at 30°C for 48 h. Then, the seeds were placed in pot sand soil and grown at 28°C under fluorescent light. Once the seedlings had about five leaves, they were sprayed with MeJA (GIBCO) every 3 h at 28°C under fluorescent light. Seedlings were also exposed to ultraviolet light. We then used leaves to analyse *LrCHS* expression by qRT-PCR following treatment.

Results

Isolation and characterization of chalcone synthase gene *LrCHS*

A combination of RT-PCR and RACE-PCR obtained the candidate *LrCHS* gene sequence. The core sequence of *LrCHS* (about 700 bp) and the longer sequence (about 1200 bp) were amplified by RT-PCR with the primer pairs of DCH-SQF1/DCHSQR2 and DCH5F/DCHSQR2, respectively (figure 2, a&f). Subsequently, the 3' sequence (about 300 bp, figure 2, b&f) was amplified with primers DCHS3R1 and DCHS3R2 by 3'RACE-PCR. Then, the 5' sequence (about 600 bp, figure 2, c&f) was amplified with primers DCHSQR1 and DCHSYR1 through 5'RACE-PCR. The full-length cDNA of the *LrCHS* gene was assembled as a 1375 bp product which contained 73 bp of the 5'UTR sequence and 1176 bp of the complete open reading frame (ORF), and 126 bp of the 3' UTR sequence (gene bank accession number: KM114220; figure 3). The ORF of the 1176 bp product encodes a polypeptide of 391 amino acids with a theoretical molecular mass of 42,798 Da and a theoretical pI of 5.807.

The full cDNA sequences of CHS that were amplified with the primers PCHSWF1 and PCHSWR1 were 1209 bp in length (figure 2d). Moreover, the genomic DNA sequences of CHS that was amplified with primers PCHSWF1/PCHSWR1 were 1860 bp in length and there was only one intron of 651 bp in length at positions +179 to +829. The coding region was divided into two parts at 178 bp and 998 bp in length (figure 3). The introns have typical characteristics of plant introns, such as a 5' splicing site with GT, a 3' splicing site with AT, and being rich in AT (74.19%).

Bioinformatic analysis of the *LrCHS* gene

Four chemically reactive residues (i.e., Cys164, Phe215, His303 and Asn336) were revealed in the *LrCHS* amino acid

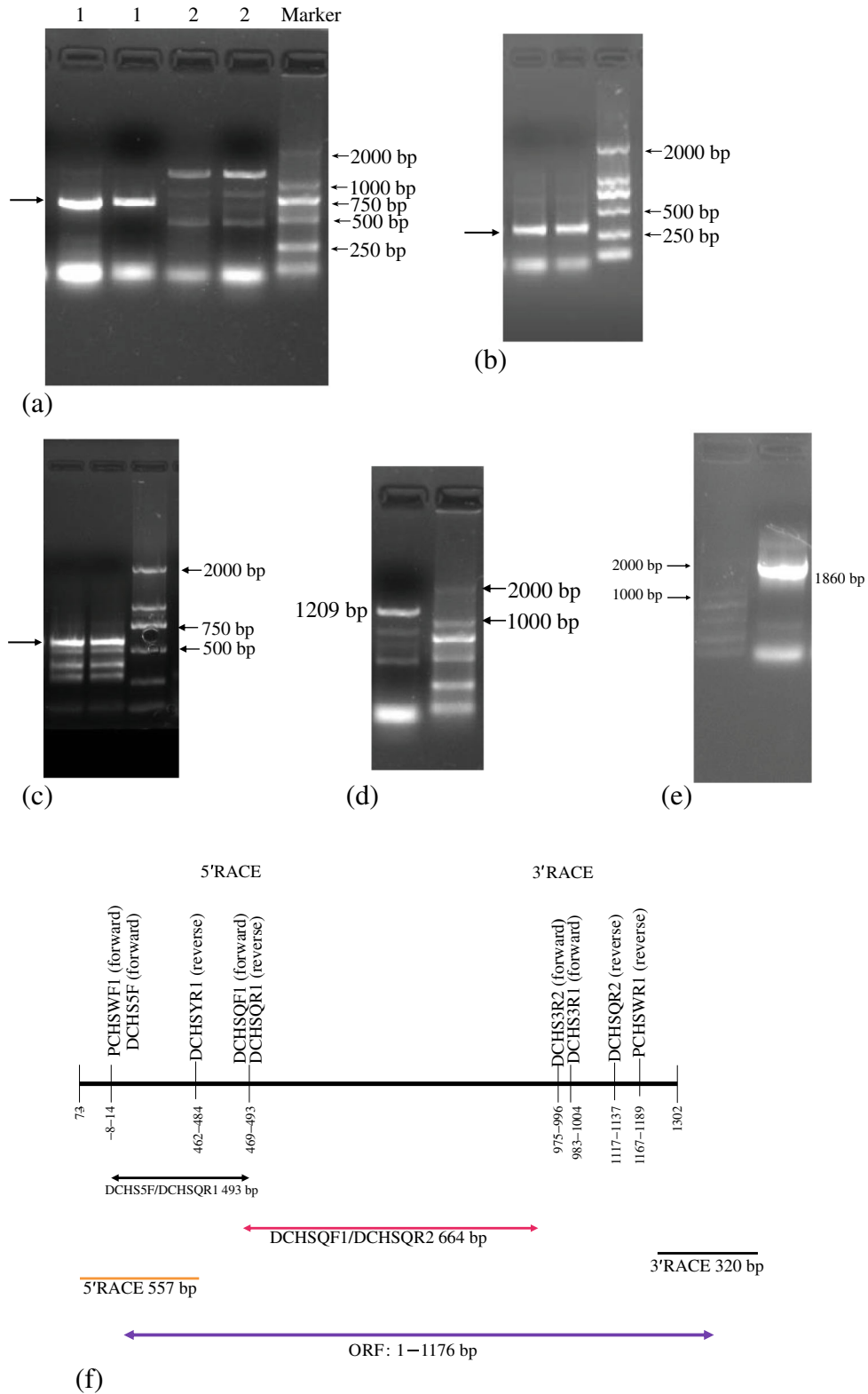


Figure 2. Isolation and identification of *LrCHS*. (a) RT-PCR products from the leaves of *L. rotata* with primers DCHSQF1/DCHSQR2 for lane 1 and DCH5F/DCHSQR2 for lane 2. Marker: DL-2000 marker. (b) 3'RACE-PCR products from the leaves of *L. rotata* with DCHS3R2/3'RACE-PCR inner primer. (c) 5'RACE-PCR products from the leaves of *L. rotata* with DCHSYR1/5'RACE-PCR inner primer. The brown signal indicated the right PCR products. (d) The full cDNA products of *L. rotata* with PCHSWF1/PCHSWR1 primers. (e) The full genomic DNA products of *L. rotata* with PCHSWF/PCHSWR primers. (f) RT-PCR and RACE-PCR product lengths with different primers.

-73 ACCCACACTACAAGCTAATAACTCCCTACTTTCCACCACCACAACCCTGTAGCAAAACAA
 -13 CTTTCCGTCGAAAAATGTGACCGTGGGAAGACATTGCGAGGGCTCAACGGGCAGAGGGTCC
 M V T V E D I R R A Q R A E G P
 48 CGCCACCGTCTTGGCCATCGGAACCGCCACCCCATCCAACCTGCGTCGATCAGAGCAGTA
 A T V L A I G T A T P S N C V D Q S T Y
 108 TCCCGATTACTATTTTCGTATCACTAATAGTGAACATATGACCGAGCTTAAAGAGAAATP
 P D Y Y F R I T N S E H M T E L K E K F
 168 TAAGCGCATGTTAAGTATTTAGTATTTAATTTTCGCAAAATTTCAATTTCTTTTGT
 K R M C
 228 CTTTTTAATTATGAAGTAGAATCTTTCGTCGTGAGATATCTCAATCAAAAAATAAAA
 288 AAATCCGGCAACAAAACATGGAGAATTAACCTTCTCAGCACATGCATGGAAGTCGTTAC
 348 GTGTACTCTTTTCTATTAGAAACATGCAATGTGCGCTGTTAAGATATAAATATATTTCAAT
 408 ACGCAATTAACCTTTTTTTTTTTTCTAATCTGATTTCTTTTTTCTACACTTACATTG
 468 CTAATTTTAAACATATGTTTACTTTGAGTTAAAAAATCTATTTTGATAACTTTCTTATT
 528 TTCCAAAAAGTCCCAAAAAACATTTAAAGTTTCTTTCAATTTAATCCAATTAATTATC
 588 TAGGCAATTTTGTAGTCCAAAGTTGGTACGTTGGGTTAAAAATTAATCTCATAATTTTTT
 648 ATTTTTTGTAAAAGTCAAGAAATATGGCACCTCAAATTCGACGATTTTATGATCATA
 708 ATTGGACCAATTAAGGAGCTATGCGATTAATTTGAAAATTTTATTTCGAAGAGAAATGGA
 768 TTTCAACACTGTTTATTTGTAATGTGTCAAATATATTTATATATTTCACATATTTGCG
 828 AGGTGAAAAATCGACTATCAATAAGCGATACATGCACCTGACGGAGGACTACCTGAAAGA
 E K S T I N K R Y M H L T E D Y L K E
 888 GAACCCGAACGCTCGCCCTACATGGCGCCGTCGCTGGACCGCCGGCAAGACCTGGTGGT
 N P N V C A Y M A P S L D A R Q D L V V
 948 GGTGGAGGTTCCGAAGCTCGGAAAAGAAGCTGCCAAAAAGCCATCAAGAATGGGGGCA
 V E V P K L G K E A A Q K A I K E W G Q
 1008 GCCCAATCGGAAGATCACCCACCTGCTCTTCTGCACCACGAGCGCGTCGACATGCCCGC
 P K S K I T H L V F C T T S G V D M P G
 1068 CGCCGACTACCAGCTACCAAGCTCCTCGGCCCTCCGCCCGCGTCAAACGCTTCATGAT
 A D Y Q L T K L L G L R P A V K R F M M
 1128 GTACCAGCAGGGCTGCTCTGACGGTGGGACTGTTCTCGCCTGGCCAAAGACTAGCGGA
 Y Q Q G C S A G G T V L R L A K D L A E
 1188 GAACAATGCCGGTGACCGGGTTTTAGCCGTTTCTCGGAGATCACCGTCATTAGTTCCG
 N N A G A R V L A V C S E I T V I S F R
 1248 CGGGCCAGTGAGGATCATTGGACAATCTGGTGGGGCAGCGTGTTCGGGGAGCGCGC
 G P S E D H L D N L V G Q A L F G D G A
 1308 TGCAGCAGTGATTGTTGGGTCGACCCCGTGGTGGGAGTGAACGACGCGTTTTCCAAC
 A A V I V G S D P V V G V E R P L F Q L
 1368 TGTCTGACGCGTGCAGACTCTTCTCCAGATTGGAAGCGTCTAATGGACATCTACG
 V S T V Q T L L P D C E A S I N G H L R
 1428 GGAGATGGGATATTTTCCAGATTCTAAAAGATGTTCTTTCTTAATATCTGAACATAT
 E M G I I F Q I L K D V P F L I S E H I
 1488 TGAGAAGAGCTGAAGGAAGCTTTTGACCCGTTGGGTATATCCGATTGGAACCTCAATCT
 E K S L K E A F D P L G I S D W N S I F
 1548 CTGGATAGCGATCCTGGTGGGCCGCAATCTTAATGGGGTCGAGCGCAAGTTAGGTCT
 W I A H P G G P A I L N G V E A K L G L
 1608 CGAGCCCGACAACCTCCGGTCGAGTAGACATGTGTTGAGTGAATATGAAACATGTTGAG
 E P D K L R S S R H V L S E Y G N M L S
 1668 TGCTTGGTGCTATTTGTGATGGATGAAATGCGAAAAGTCTCCGCAATGAAGGGCGGAG
 A C V L F V M D E M R K V S A N E G R S
 1728 CTCCACCGGGGAAGGGCTGGATTGGGGCGTACTCCTTGGATTCCGGCCGGGCTGACCAT
 S T G E G L D W G V L L G F G P G L T I
 1788 TGAGACAGTCTGCTGCACAGTGCACAATCACTAATTAATATGGTTACTTAATTTGACT
 E T V V L H S V P I T N
 1848 ACGGGTTCGGACTCTATGCATTAAGAAAAGTGGAAAATGAATTAATAAATTAATGAAATA
 1908 ATAACATGGCAGCCTGATGTAGACGCGTTGATCCAAAAAATAAAAA

Figure 3. Genomic DNA sequence and deduced amino acid sequence of the *CHS* gene from *L. rotata*. The transcription start site (ATG) is underlined. The sequence in the box is one intron with 651 bp.

sequences (figure 3), which are conserved in all known CHS-related enzymes, and define the active site. Five residues (i.e., Ser133, Glu192, Thr194, Thr197(S) and Ser338(L)) formed the coumaroyl-binding pocket, and seven residues (i.e., Thr132, Met137, Phe215, Ile254, Gly256, Phe265 and Pro375) formed the cyclization pocket (Ferrer *et al.* 1999; Dao *et al.* 2011). Moreover, all CHS-like proteins exhibited strong conservation of residues that shape the geometry of the active site (i.e., Pro138, Gly163, Gly167, Leu214, Asp217, Gly262, Pro304, Gly305, Gly306, Gly335, Gly374, Pro375 and Gly376) (Ferrer *et al.* 1999). In CHS, Phe215, which is conserved in all type III PKSs as the ‘gate-keeper’ is located at the junction between the active-site cavity and the CoA binding tunnel. It is thought to facilitate the decarboxylation of malonyl-CoA and to help orientate the substrates and intermediates during condensation reactions (Ferrer *et al.* 1999).

The LrCHS protein was CHS-like in other plants according to BLAST analysis. As predicted, LrCHS was a soluble protein, located in the cellular cytoplasm and contained two global domains. The secondary LrCHS structure consisted of random coils, α -helices and extended strands, with the former two being the predominant components. Two-dimensional modelling revealed that LrCHS consisted of 26.85% α -helix, 11.00% extended strand and 18.93% random coil. The α -helices were distributed as four clusters in the N-terminal domain and in the middle. The extended strand was distributed as three and four clusters in the N-terminal and in the middle, respectively. The random coil was distributed at most LrCHS protein regions. Most of the recognized motifs occurred in the coiled-coil LrCHS structure, which was consistent with the fact that coiled-coils generally contain most of the significant motifs associated with biological functions of various proteins. LrCHS thus, had the typical molecular structure of CHS and compared well with the experimental data for *M. sativa* CHS (Ferrer *et al.* 1999).

The computationally modelled three-dimensional structure of CHS from *L. rotata* is shown in figure 4. Additionally, the 3D structural modelling and phylogenetic analysis indicated that LrCHS and CHS from *Agastache rugosa* were closely related (figures 5 and 6), which indicated that LrCHS is a homolog of the CHS gene, and its protein is a typical CHS protein.

Phylogenetic analysis

We aligned nucleotide sequences with the DNAssist program (software ver. 2.1), and performed BLAST searches (see <http://www.ncbi.nlm.nih.gov>). *LrCHS* showed higher identities (i.e., 79–80% on nucleotide level) with CHS of *Agastache rugosa* (JQ314450), *Perilla frutescens* (AB002582) and *Perilla frutescens* (AB002815). Alignment of protein sequences is shown in figure 5. The *LrCHS* shared 86% sequence identity with the CHS proteins of *Solenostemon scutellarioides* (GenBank accession number

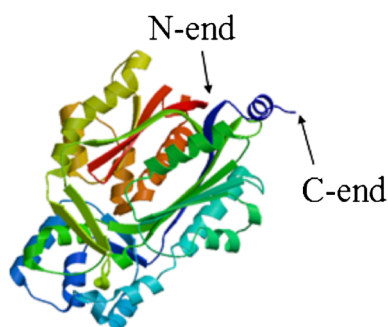


Figure 4. The computationally modeled three-dimensional structure of the CHS protein from *L. rotata*.

ABP57071.1), *Perilla frutescens* (GenBank accession number BAA19656.1) and *Agastache rugosa* (GenBank accession number AFL72079.1), 85% with a CHS of *Misopates orontium* (GenBank accession number CAJ44127.1), 82% with a CHS of *Solanum tuberosum* (GenBank accession number AEN83501.1) and 81% with a CHS of *Rhus chinensis* (GenBank accession number AGH13332.1).

The fully aligned CHS amino acid sequences from 44 plants containing nine families (table 2) were used to generate a minimum evolution tree using Poisson correction measurements. The resulting trees are shown in figure 6. The CHS proteins were shown to cluster 9 dependent branches of nine different families by the minimum evolution method (figure 6). For example, all the *Solanaceae* plants gathered on one tree branch. As expected, *L. rotata* was closely related to *Lamiaceae* with bootstrap support (75%; figure 6). *L. rotata*, *Agastache rugosa*, *Solenostemon scutellarioides*, *Perilla frutescens* and *Scutellaria baicalensis*, belong to the family *Labiatae*, and form one tree branch, which is attributed to higher amino acid sequence identity. As shown in figure 6, *Labiatae* showed the closest relationship to *Scrophulariaceae*, but was farthest from *Poaceae* and *Polygonaceae*. In addition, it should be expected that *L. rotata* belongs to *Labiatae* based on the phylogenetic tree that was derived from CHS amino acid sequences.

Divergence of *LrCHS* expression among different organizations in *L. rotata*

We examined the *LrCHS* expression pattern in different tissues using total RNA from leaves, stems, roots, petioles and the flower petals. The qRT-PCR analyses are shown in figure 7. *LrCHS* transcription was clearly tissue specific and developmentally dependent. The highest *LrCHS* mRNA level was observed in flowers, with moderate levels in petioles; however, *LrCHS* expression was lowest in the stems. The *LrCHS* transcript was expressed from strong to weak in the following order: flowers > leaves > petioles > roots > stems. The highest *LrCHS* expression occurred in flowers, which apparently corresponded to petal pigmentation and may be responsible for anthocyanin biosynthesis in petals

(Mary et al. 2000; Huang et al. 2012). Considering the low *LrCHS* expression levels in stem tissues, it may not be the major site of CHS gene expression for anthocyanin biosynthesis. These results suggest that tissue specificity of CHS gene expression in *L. rotata* is variable, and further suggests considerable divergence in the developmental regulation of individual gene family members.

Total flavonoid content

Chalcone synthase catalyses the initial step in flavonoid synthesis. Moreover, flavonoid content was related to CHS gene expression. During *L. rotata* organization, total flavonoid content changed during different *L. rotata* organizations (figure 8). Total flavonoid content was expressed from a strong to a weak order thus: flowers > leaves > petioles > roots > stems. The highest total flavonoid content was observed in flowers, where it was up to 7.38 mg/g. Total flavonoid content was 6.3 mg/g in leaves, and the minimum content in stems reached a level of 1.39 mg/g. These results show that tissue specificity of total flavonoid content in *L. rotata* was quite variable, suggesting a similar trend as seen with CHS expression.

Expression profile of *LrCHS* following exposure to MeJA and UV

Short-term exposure to MeJA increases baicalin expression, whereas long-term exposure inhibits plant cell growth (Zhang and Xu 2006). We used qRT-PCR with primers DCH-SYF1/DCHSYR1 to study changes in *LrCHS* expression following exposure to MeJA and UV (figure 9). After treatment with MeJA and UV, *LrCHS* expression was stimulated after a 6–18 h exposure and peaked after 12 h. *LrCHS* expression showed a decreasing trend after 24–36 h of treatment (figure 9). This indicated that *LrCHS* expression was sensitive to MeJA and UV, and that *LrCHS* levels may be modulated by these two treatments. Enhanced *LrCHS* expression in the presence of MeJA and UV would be expected to augment CHS activity and the accumulation of plant secondary metabolites in *L. rotata*. This agrees with Sánchez-Sampedro et al. (2005), who observed that MeJA enhanced CHS activity and increased silymarin levels in *Silybum marianum* cell cultures.

Discussion

We identified a novel homologue of chalcone synthase *LrCHS* in seedling extracts of *L. rotata*. Sequence analysis and comparison with *L. rotata* CHS revealed that the ORF was 1176 bp in length and putatively encoded a polypeptide of 391 amino acids, which had high similarities (80–86%) with CHSs from other plant species, a predicted molecular mass of 42.8 kDa, and a pI of 5.8. A putative amino acid sequence analysis revealed that *L. rotata* CHS contained active amino-acid residues that are highly conserved among

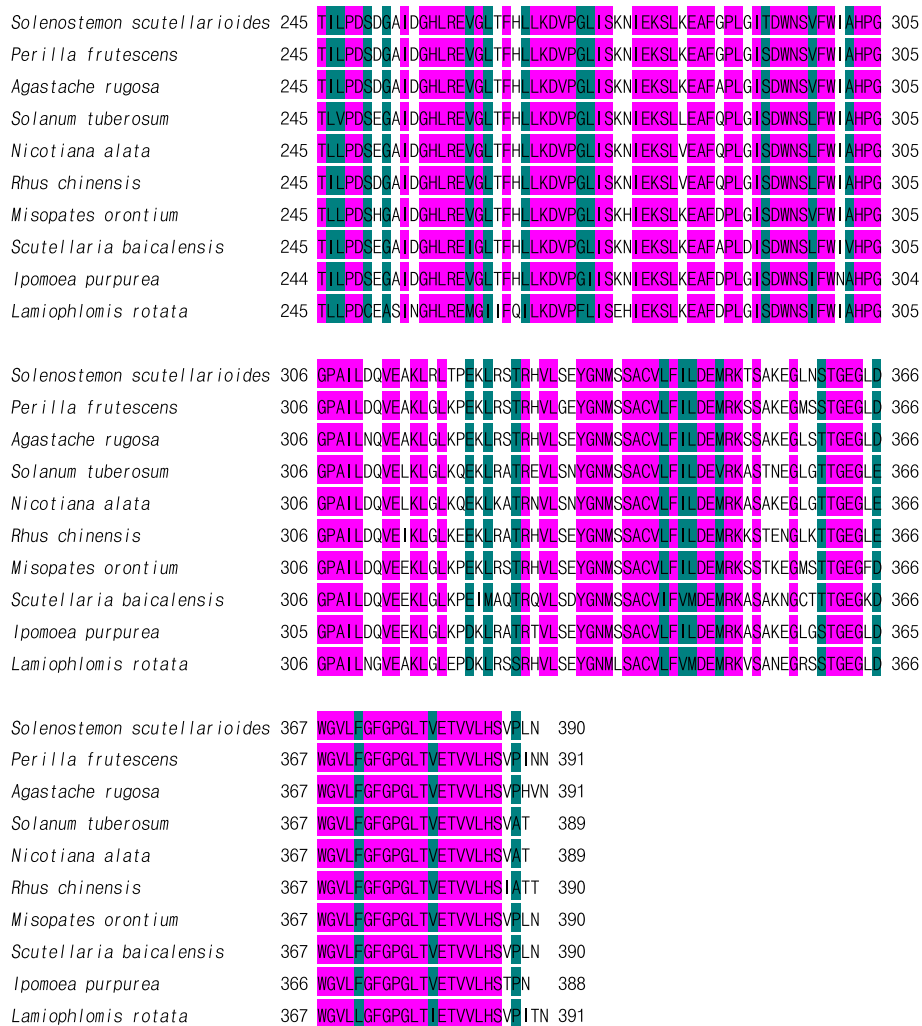


Figure 5. Multiple sequence alignment of LrCHS and other plant CHS proteins. Identical sites are shown in black letters on rose red background; conserved sites with only one different site are shown in black letters on a deep green background. Other sites are shown in black letters on a white background. The database accession numbers of the sequences used in the alignment are: *Solenostemon scutellarioides* (*ScCHS*, GenBank accession no. ABP57071.1), *Perilla frutescens* (*PfCHS*, GenBank accession no. BAA19656.1), *Agastache rugosa* (*ArCHS*, GenBank accession no. AFL72079.1), *Solanum tuberosum* (*StCHS*, GenBank accession no. AEN83501.1), *Nicotiana alata* (*NaCHS*, GenBank accession no. ACS12837.1), *Rhus chinensis* (*RcCHS*, GenBank accession no. AGH13332.1), *Misopates orontium* (*MoCHS*, GenBank accession no. CAJ44127.1), *Scutellaria baicalensis* (*SbCHS*, GenBank accession no. AAB88208.1), *Ipomoea purpurea* (*IoCHS*, GenBank accession no. BAA20387.1) and *L. rotata* (*LrCHS*, GenBank accession no. KF385880).

a major role in the cyclization reaction from chalcone to flavanone. In this study, qRT-PCR analysis (figure 7) demonstrated that the pattern of *CHS* gene expression in *L. rotata* organs was correlated with that of flavonoid content. The relevant flavonoid metabolizing enzyme activities at this period contributed to high flavonoid content (figure 8). The total flavonoid content and *CHS* gene expression exhibited similar patterns during *L. rotata* organ development. We suggest that *CHS* is regulated at the transcriptional level, and thus, it may contribute to the accumulation of total flavonoids in *L. rotata*.

Chalcone synthase is a key enzyme of the flavonoid and isoflavonoid biosynthetic pathway. Indeed, *CHS* gene

expression is influenced by many stress and environmental factors such as UV irradiation, wound repair, or pathogen attack (Dixon and Paiva 1995; Ito et al. 1997; Zhou et al. 2013). It also provides the starting materials for a diverse set of genes, which have differentially important roles in flowering plants, like provision of floral pigments, antibiotics, UV protectants, and insect repellents (Hahlbrock and Scheel 1989). In this study, *CHS* gene expression was induced in *L. rotata* under stressful conditions such as UV light and MeJA over a short time. *CHS* expression may cause metabolite (flavonoid) accumulation and might thus be involved in UV light and the MeJA defense pathway.

A chalcone synthase gene from L. rotata

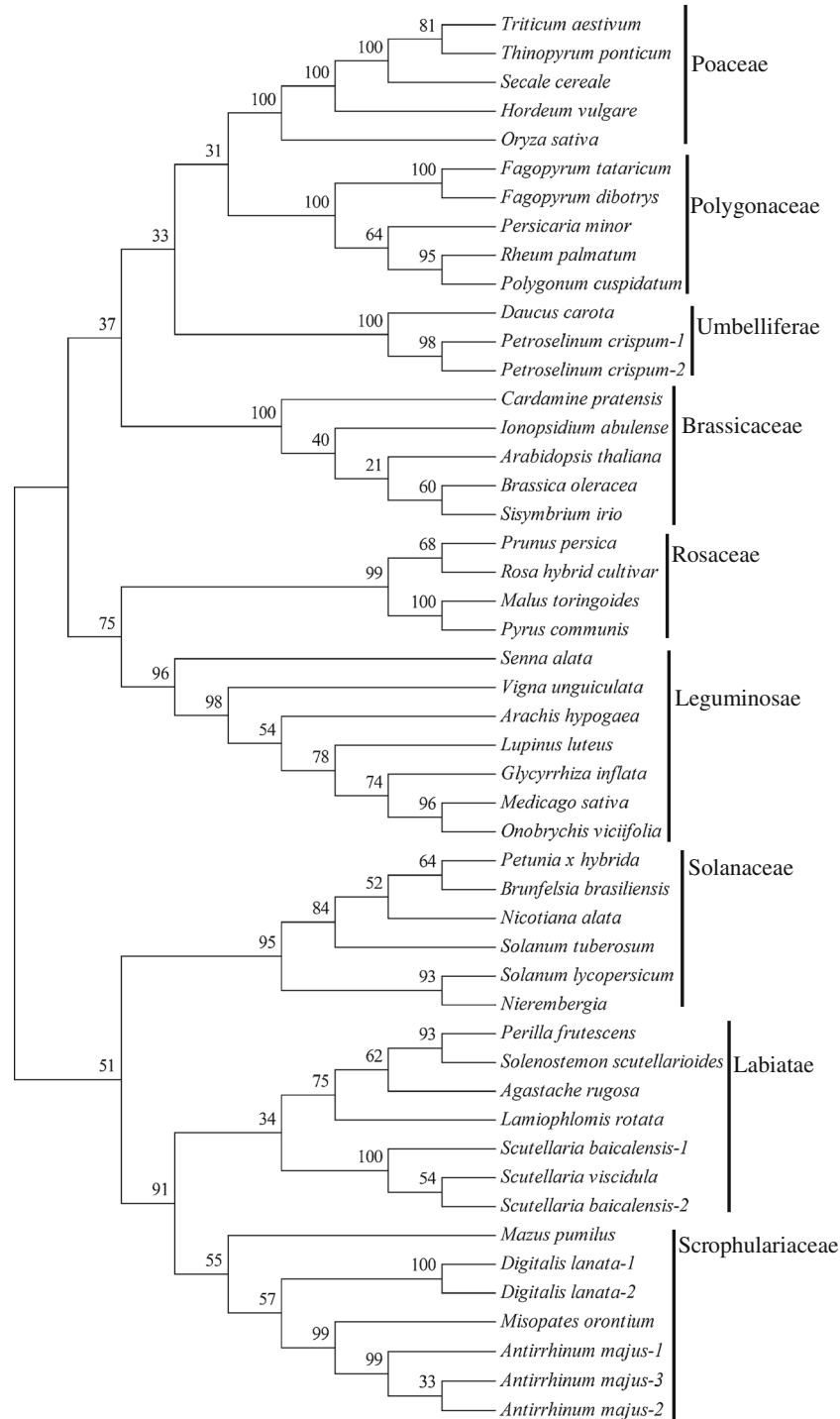


Figure 6. Phylogenetic analysis of plant and *L. rotata* CHS. The phylogenetic tree was constructed by the minimum evolution method (based on 1000 bootstrap replicates) using the MEGA4.1 software; the bootstrap values are shown on the branches. The database accession numbers of the sequences used are provided in table 2.

In summary, we have cloned and characterized an *LrCHS* gene from the medicinal herb *L. rotata*. The protein encoded by this gene (*LrCHS*) shares various structural similarities with the corresponding proteins from other plants, especially *Agastache rugosa*, including a binding site form

alonyl-CoA and an N-myristoylation motif. These structural similarities suggest that *LrCHS* may be involved in plant intermediate metabolism. Additionally, qRT-PCR showed that *LrCHS* was responsive to MeJA and UV light at the transcriptional level, which might provide an

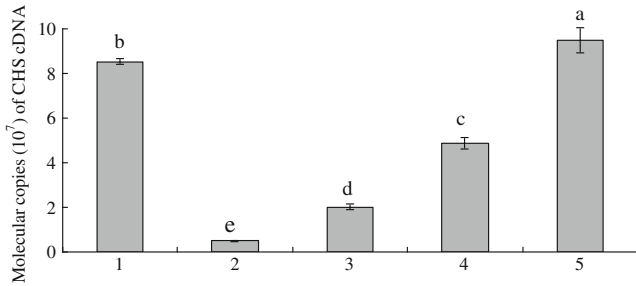


Figure 7. Expression profile of *LrCHS* in different tissues. Data represents the mean values of five replicates (\pm SD). The copy number of CHS cDNA in different organizations of *L. rotata*. 1, leaves; 2, stems; 3, roots; 4, petioles; 5, flowers. The different subscriptions with different letters indicate significant difference ($P < 0.05$).

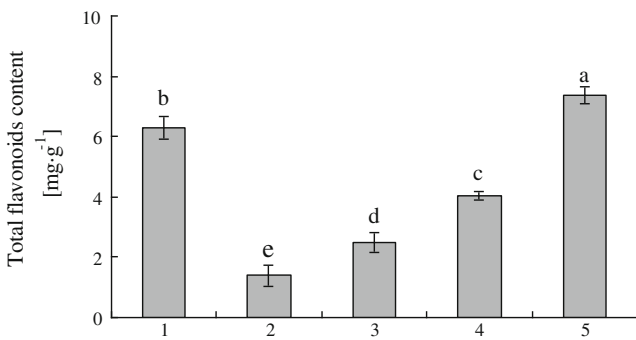


Figure 8. Changes in total flavonoid content during different organizations of *L. rotata*. 1, leaves; 2, stems; 3, roots; 4, petioles; 5, flowers. The data were the means from three separate experiments. Bars are standard errors ($n = 3$). The different subscriptions with different letters indicate a significant difference ($P < 0.05$).

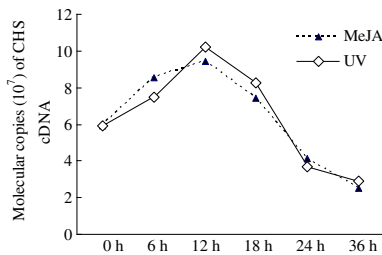


Figure 9. Expression profile of *LrCHS* following exposure to MeJA and UV for different lengths of time.

important mechanism to enhance intracellular flavonoid levels. These results provide useful information on the induction and regulation of genes involved in flavonoid biosynthesis.

References

Abdel-Lateif K., Vaissayre V., Gherbi H., Verries C., Meudec E., Perrine-Walker F. et al. 2013 Silencing of the chalcone synthase gene in *Casuarina glauca* highlights the important role of flavonoids during nodulation. *New Phytol.* **199**, 1012–1021.

Alfred B., Bruno E. and Eberhard S. 1991 Cloning and characterization of a chalcone synthase gene from mustard and its light-dependent expression. *Plant Mol. Biol.* **16**, 175–185.

An C. C., Ichinose Y., Testuji Y., Shiraishi T. and Oku H. 1993 Organization of the genes encoding chalcone synthase in *Pisum sativum*. *Plant Mol. Biol.* **21**, 789–803.

Commenges D., Scotet V., Renaud S., Jacqmin-Gadda H., Barberger-Gateau P. and Dartigues J. F. 2000 Intake of flavonoids and risk of dementia. *Eur. J. Epidemiol.* **16**, 357–363.

Dao T. T., Linthorst H. J. M. and Verpoorte R. 2011 Chalcone synthase and its functions in plant resistance. *Phytochem. Rev.* **10**, 397–412.

Dare A. P. and Hellens R. P. 2013 RNA interference silencing of CHS greatly alters the growth pattern of apple (*Malus x domestica*). *Plant Signal Behav.* **8**, e25033.

Dixon R. A. and Paiva N. 1995 Stress-induced phenylpropanoid metabolism. *Plant Cell* **7**, 1085–1097.

Dooner H. K. 1983 Coordinate genetic regulation of flavonoid biosynthetic enzymes in maize. *Mol. Gen. Genet.* **189**, 136–141.

Dugas A. J., Castaneda-Acosta J., Bonin G. C., Price K. L., Fischer N. H. and Winston G. W. 2000 Evaluation of the total peroxyl radical-scavenging capacity of flavonoids: structure activity relationships. *J. Nat. Prod.* **63**, 327–331.

Edwards M. L., Stemerick D. M. and Sunkara P. S. 1990 Chalcones: a new class of antimetabolic agents. *J. Med. Chem.* **33**, 1948–1954.

Ferrer J. L., Jez J. M., Bowman M. E., Dixon R. A. and Noel J. P. 1999 Structure of chalcone synthase and the molecular basis of plant polyketide biosynthesis. *Nat. Struct. Biol.* **6**, 775–784.

Gehm B. D., McAndrews J. M., Chien P. Y. and Jameson J. L. 1997 Resveratrol, a polyphenolic compound found in grapes and wine, is an agonist for the estrogen receptor. *Proc. Natl. Acad. Sci. USA* **94**, 14138–14143.

Hahlbrock K. 1981 Flavonoids. In *Biochemistry of plants* (ed. P. K. Stumpf and E. E. Conn), pp. 425–456. Academic Press, New York, USA.

Hahlbrock K. and Scheel D. 1989 Physiology and molecular biology of phenylpropanoid metabolism. *Annu. Rev. Plant Physiol. Plant Mol. Biol.* **40**, 347–369.

Heller W. and Hahlbrock K. 1980 Highly purified ‘flavanone synthase’ from parsley catalyzes the formation of naringenin chalcone. *Arch. Biochem. Biophys.* **200**, 617–619.

Huang L., Wang H., Ye H., Du Z., Zhang Y., Beerhues L. et al. 2012 Differential expression of benzophenone synthase and chalcone synthase in *Hypericum sampsonii*. *Nat. Prod. Commun.* **7**, 1615–1618.

Ito M., Ichinose Y., Kato H., Shiraishi T. and Yamada T. 1997 Molecular evolution and functional relevance of the chalcone synthase genes of pea. *Mol. Gen. Genet.* **255**, 28–37.

Jang M. S., Cai L. N., Udeani G. O., Slowing K. V., Thomas C. F., Beecher C. W. W. et al. 1997 Cancer chemo preventive activity of resveratrol, a natural product derived from Grape. *Science* **275**, 218–220.

Jiang C. G., Schommer C. K., Kim S. Y. and Suh D. Y. 2006 Cloning and characterization of chalcone synthase from the moss, *Physcomitrella patens*. *Phytochemistry* **67**, 2531–2540.

Li R. S., Kenyon G. L., Cohen F. E., Chen X. W., Gong B. Q., Dominguez J. N. et al. 1995 *In vitro* antimalarial activity of chalcones and their derivatives. *J. Med. Chem.* **38**, 5031–5037.

Liu J. M. 2006. Genetic diversity and lipophilic composition in *Lamiophlomis rotata*, an endemic species of Qinghai-Tibetan plateau. *Fudan University*, Doctor dissertation.

Lu X., Zhou W. and Gao F. 2009 Cloning, characterization and localization of CHS gene from blood orange, *Citrus sinensis* (L.) Osbeck cv. Ruby. *Mol. Biol. Rep.* **36**, 1983–1990.

Lü W. J., Li M. X., Chen Y. L., Chen H. L. and Chen X. G. 2012 Simultaneous determination of iridoid glycosides and flavonoids in *Lamionophlomis rotata* and its herbal preparation by a simple

- and rapid capillary zone electrophoresis method. *Drug Test Anal.* **4**, 123–128.
- Mary L. D., Bonnie M. C. and Michael T. C. 2000 Molecular evolution of the chalcone synthase multigene family in the morning glory genome. *Plant Mol. Biol.* **42**, 79–92.
- McKhann H. I. and Hirsch A. M. 1994 Isolation of chalcone synthase and chalcone isomerase cDNAs from alfalfa (*Medicago sativa* L.): highest transcript levels occur in young roots and root tips. *Plant Mol. Biol.* **24**, 767–777.
- Murray M. G. and Thompson W. F. 1980 Rapid isolation of high molecular weight plant DNA. *Nucleic Acids Res.* **8**, 4321–4325.
- Nakajima O., Shibuya M., Hakamatsuka T., Noguchi H., Ebizuka Y. and Ushio Sankawa U. 1996 cDNA and genomic DNA clonings of chalcone synthase from *Pueraria lobata*. *Biol. Pharm. Bull.* **19**, 71–76.
- Pang Y. Z., Shen G. A., Liu C. H., Liu X. J., Tan F. and Sun Y. 2004 Molecular cloning and sequence analysis of a novel chalcone synthase cDNA from *Ginkgo biloba*. *DNA Seq.* **15**, 283–290.
- Pitakdantham W., Sutabutra T., Chiemsombat P. and Pitaksutheepong C. 2010 Isolation and characterization of *chalcone synthase* gene isolated from *Dendrobium Sonia Earsakul*. *Pak. J. Biol. Sci.* **13**, 1000–1005.
- Sánchez-Sampedro M. A., Fernández-Tárrago J. and Corchete P. 2005 Yeast extract and methyl jasmonate-induced silymarin production in cell cultures of *Silybum marianum* (L.) Gaertn. *J. Biotechnol.* **119**, 60–69.
- Sugihara N., Arakawa T., Ohnishi M. and Furuno K. 1999 Anti- and pro-oxidative effects of flavonoids on metal-induced lipid hydroperoxide dependent lipid peroxidation in cultured hepatocytes loaded with algalinolenic acid. *Free Radic. Biol. Med.* **27**, 1313–1323.
- Thompson J. D., Gibson T. J., Plewniak F., Jeanmougin F. and Higgins D. G. 1997 The CLUSTAL-X windows interface: flexible strategies for multiple sequence alignment aided by quality analysis tools. *Nucleic Acids Res.* **25**, 4876–4882.
- Trevisanato S. I. and Kim Y. I. 2000 Tea and health. *Nutr. Rev.* **58**, 1–10.
- Wolfe K., Wu X. and Liu R. H. 2003 Antioxidant activity of apple peels. *J. Agr. Food Chem.* **51**, 609–614.
- Zhang J. J. and Xu M. J. 2006 Effects of nitric oxide and methyl jasmonate on the baicalin production and cell growth in suspension cultures of *Scutellaria baicalensis*. *Chinese Bull. Bot.* **23**, 374–379.
- Zhou B., Wang Y., Zhan Y., Li Y. and Kawabata S. 2013 Chalcone synthase family genes have redundant roles in anthocyanin biosynthesis and in response to blue/UV-A light in turnip (*Brassica rapa*; *Brassicaceae*). *Am. J. Bot.* **100**, 2458–2467.
- Zwaagstra M. E., Timmerman H., Tamura M., Wadak Y., Onogim K. and Zhang Q. 1997 Synthesis and structure activity relationships of carboxylated chalcones: a novel series of CysLT1 (LTD4) receptor antagonists. *J. Med. Chem.* **40**, 1075–1089.

Received 13 June 2014, in revised form 14 October 2014; accepted 27 October 2014

Unedited version published online: 29 October 2014

Final version published online: 20 May 2015